2D OOPIC Simulations of the Helicon Double Layer

IEPC-2007-146

Presented at the 30th International Electric Propulsion Conference, Florence, Italy
September 17-20, 2007

I. Musso*
Center for Studies and Activities for Space, University of Padua, Padova, Italy
Institute of Information Science and Technology, National Research Council of Italy, Pisa, Italy

M. Manente†
Center for Studies and Activities for Space, University of Padua, Padova, Italy

J. Carlsson‡
Tech-X Corporation, Boulder Colorado, USA

C. Bramanti§
European Space Research and Technology Center, European Space Agency, Noordwijk, The Netherlands

and

D. Pavarin**
Center for Studies and Activities for Space, University of Padua, Padova, Italy

Abstract: The Australian National University and the Ecole Polytechnique in Palaiseau obtained experimental results of current free helicon double layer (DL) originating with electropositive and electronegative gases. The experimental evidence of the double layer envisages tantalizing performance of a thruster exploiting this effect. The paper is intended to present part of the results obtained by a deep numerical investigation on Double layer formation, stability and characteristic and to explore the applicability of this concept to space mission. The analysis has been conducted using XOOPIC, a 2-D numerical code of Berkeley University. We focused our study on the analysis of the following aspects: effects of the source walls characteristics and geometry, DL formation and stability, influence of magnetic field and neutral pressure, ions' beam divergence and flux detachment. We found that for higher neutral pressures the potential jump reduces whereas an electrically biased wall can increase its amplitude. The thrust and specific impulse have been evaluated for a low density discharge. The 2-D code results are here presented and compared with experimental data provided in literature.

Nomenclature

DL = double layer
λd = Debye length

* ISTI-CNR via Moruzzi 1, 56124, Pisa, Italy, ivano.musso@isti.cnr.it
† CISAS, via Venezia 15, 35131, Padova, Italy, marco.manente@unipd.it
‡ Tech-X Corp., Arapahoe Ave 5621, Suite A, 80303 Boulder Colorado, USA, johan@txcorp.com
§ ESA-ESTEC, Keplerlaan 1 Postbus 299, 2200 AG Noordwijk, The Netherlands, cristina.bramanti@esa.int
** CISAS, via Venezia 15, 35131, Padova, Italy, daniele.pavarin@unipd.it

RFEA = retarded field energy analyzer
PIC = particle in cell
OOPIC = object oriented particle in cell code
ANU = Australian National University
LPTP = Laboratoire de Physique et Technologie des Plasmas
IEDF = ion energy distribution function

I. Introduction

THIS paper describes results of the numerical simulations of the Helicon Double Layer (DL) performed by the authors. The electric Double Layer (DL) is the boundary discontinuity between two different plasmas, one of higher density, higher electron temperature and one of a lower density, lower electron temperature. The DL is represented by a sudden drop in plasma potential at this boundary. During the last few years, this phenomenon has been registered under different conditions and configurations by several researchers around the world. In particular, at the laboratories of the Australian National University (ANU) DL has been measured and successively reproduced in France by the Ecole Polytechnique in Palaiseau, Laboratoire de Physique et Technologie des Plasmas (LPTP). They shown the existence of a new phenomenon where a narrow potential jump occurred across H or Ar plasmas. In this case, the high density plasma is in the source tube sustained by a helicon discharge, and the low density plasma is present external to the open end of the tube and attached where the confining magnetic field diverges. DLs have also been measured without a magnetic field by using electronegative gas (Ar/SF_6) mixtures in a similar device. In both cases, the potential drop of the DL accelerates the higher density plasma in the source to supersonic speeds to form an ion beam, creating thrust at moderate exhaust velocity.

The main purpose of the present paper is to verify conditions for the DL formation, study its electrical properties and the opportunity to utilize the concept as space thruster. This type of thruster would have the additional advantage of requiring no high-current cathode, acceleration grids or neutraliser that presently limit the operating lifetime in other electric thrusters, thus they would appear suitable for very high total impulse missions.

Our analysis has been performed utilizing a free code of the Berkeley University called Object Oriented Particle In-Cell Code (OOPIC) which we choose for its versatility and stability. Next sections give a overview of the measurements to be reproduced, followed by a brief description of the software we used. Successively we describe the results of our study starting from a campaign of simulations with low density plasma, that are easier to perform because require lower memory and computational time, where we evaluated the effects of the main border conditions. The most interesting simulations than have been reproduced with higher densities by using a finer grid and comparing the results with the experimental data. Finally we analyzed the ions detachment and we evaluated the thrust and specific impulse.

II. Experiment

Charles and Boswell[1,2,3] of the Australian National University (ANU) have first reported about a current-free DL obtained by a helicon-source plasma expansion along a diverging magnetic field. The phenomenon was

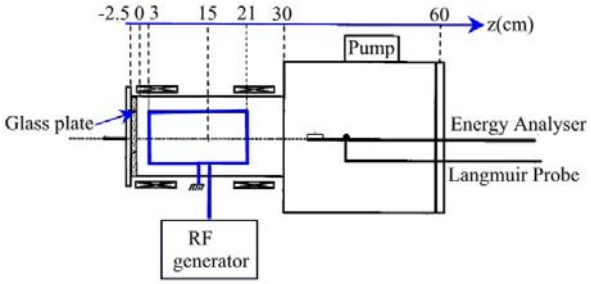

Figure 1: ANU Chi Kung system. *The horizontal helicon device utilized by Charles.*

accompanied by an ion beam at axial velocities two times the ion sound speed, as seen by using a Retarded Field Energy Analyzer (RFEA). The potential jump appeared just inside the helicon, for neutral pressures below 3 mTorr and for axial magnetic fields grater than 120 Gauss inside the source tube. It had an amplitude of almost 20 V and it was few centimeters large. Fig 1 reproduces the experimental apparatus used at ANU laboratories and Fig 2 shows the main measurements they have done.

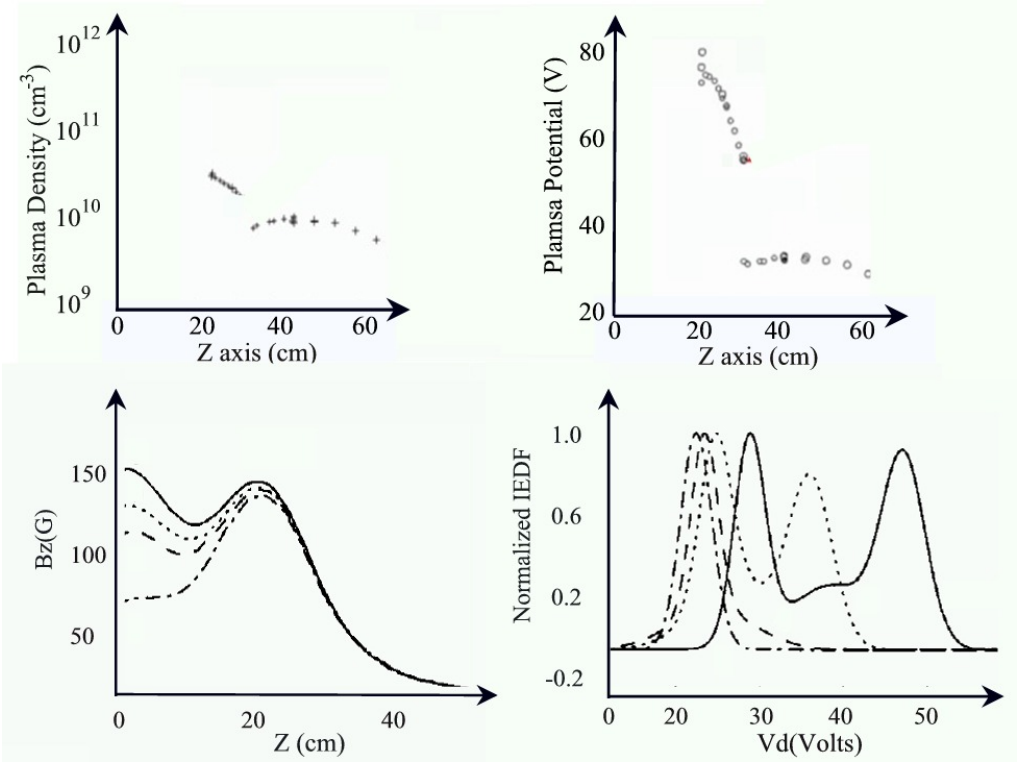

Figure 2. Measurements made by Charles at the ANU laboratories. *The potential jump appeared near the source/chamber interface. Inside the diffusion chamber (z=40 cm) IEDF have been measured showing a double peak distribution. The axial velocity of the ions responsible for the second peak of the function was evaluated around two times the ion sound speed. This high energy ions disappeared with lower magnetic fields.*

Plihon[4,5] reproduced the Charles results and demonstrated the existence of the helicon DL also without axial magnetic field when trace of electronegative ions are mixed with the electropositive ones. Ions flux enhancing has been reported when biased left source walls were used.

III. Model description

OOPIC (Object-Oriented Particle-In-Cell) is a 2D-3V relativistic electromagnetic PIC code, open-source of Berkeley University[6]. One of the principal advantages of the object-oriented method is the potential for rapid extension and enhancement of the code. The X11 version, called XOOPIC, uses the XGrafix package and additional diagnostics can be defined without recompiling the code. The applicability of this code ranges from plasma discharges, such as glow and RF discharges, to microwave-beam devices. The boundaries can be determined at runtime and include many models of emitters, collectors, wave boundary conditions and equipotentials. The code can handle an arbitrary number of species and it includes Monte Carlo collision (MCC) algorithms for modeling collisions of charged particles with a variety of neutral background gas.

Because the dependence on the azimuthal angle is not expected to be relevant for DL experiments, we can use a 2D r-z cylindrical PIC simulation. Modeling the Charles' experiment we must draw a first dielectric open-ended

cylinder connected to a conducting one, representing the source and diffusion chamber walls. The source and chamber radiuses are 6 and 16 cm while the length is 30 cm for both. We implemented a half thruster stressing its cylindrical symmetry (Fig 3).

The static magnetic field has been calculated by solving the equations for circular filamentary coils. The two solenoids of the Charles and Plihon experiments are located around the source tube. Their dimensions have been extrapolated from the figures of the ANU and LPTP publications.

The particles are created at a given rate in a rectangular area and with Maxwellian velocity distribution and a changeable density distribution. The plasma production density is defined in order to model the typical helicon source behavior: maximum density near r=0 and after half of the tube (Fig 3).

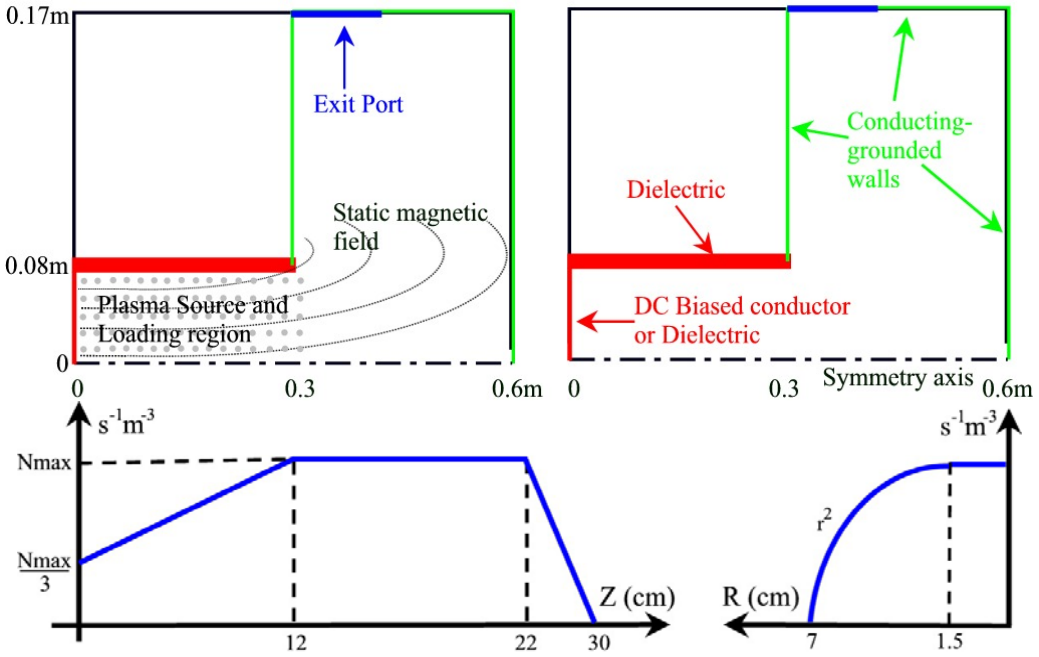

Figure 3. OOPIC model and plasma production function. *The model reproduced the experimental geometry and dimensions. The walls have been shaped by using OOPIC objects: conducting grounded segments for the diffusion chamber and dielectric or conducting electrically biased surfaces for the helicon source. The plasma production area is located inside the helicon tube and its distribution function has been drawn with a maximum at the axis and after half of the source.*

Table 1: Reference parameters

Particles	**H**	**Neutral Density (mT)**	**1.6**
Magnetic field (G)	**125**	**Time Step (s)**	**10^{-9}**
Macro-part relative weight	**10^{3}**	**Duration (μs)**	**11**
R Space Step (mm)	**1.2**	**Z Space Step (mm)**	**1.2**
PRODUCED PARTICLES		**IMMEDIATELY LOADED PARTICLES**	
Te (eV)	**7**	**Te (eV)**	**10**
Ti (eV)	**0.5**	**Ti (eV)**	**0.5**
Source Rate (s^{-1} m^{-3})	**5 10^{17}**	**Density (m^{-3})**	**10^{9}**

IV. Sparse grid simulations

The first analysis have been done by considering low plasma densities: this permits to reduce the particles' number and the spatial grid, which is scaled with λd, and the dimension of the fields' matrixes that consequently OOPIC can manipulate without the need of a supercomputer in a reasonable time. The time step has been set at 10^{-9}s

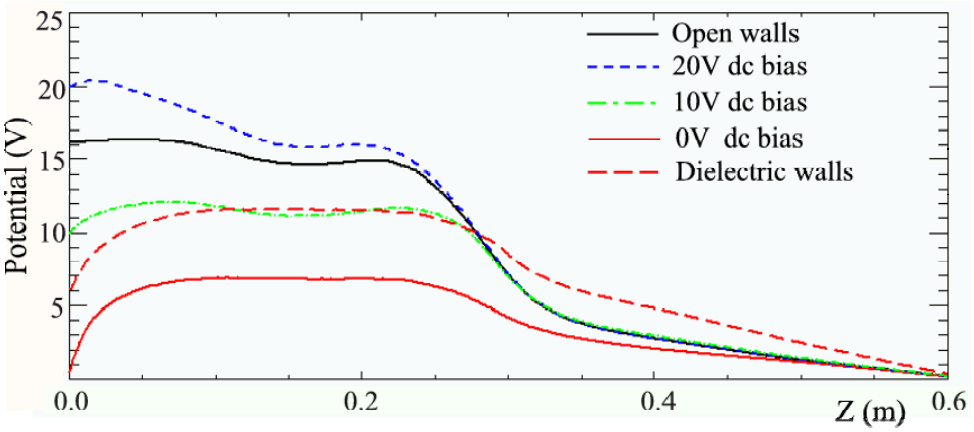

Figure 4. Source walls effects. *After 11μs the potential jump near the source/chamber interface is almost 10V. The maximum plasma potential is obtained when the left wall is defined as conducting and biased at 20V. The dielectric wall provide values lower than the open wall. Final density* N_{ions}*~5* 10^{12} m^{-3}.

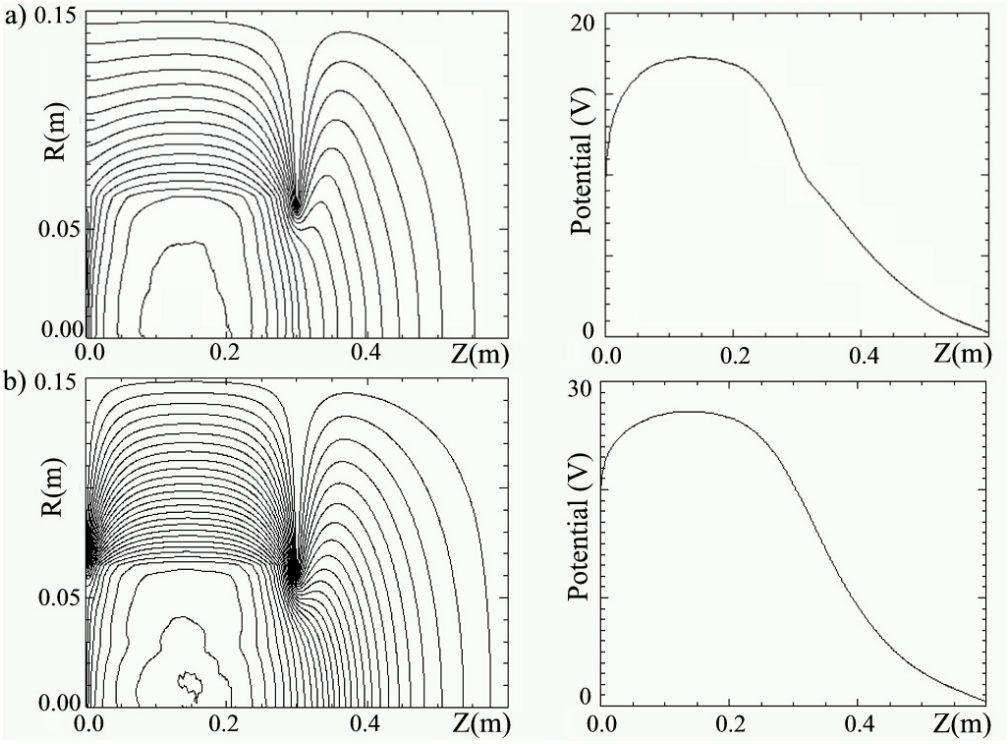

Figure 5: Plasma electric potential for dielectric and conducting left source walls. *The picture represents the electric equipotential lines and the axial potential for dielectric (a) and conducting 20 Volts biased left source walls (b).*

in accordance with the electron cyclotron and plasma frequencies and a comparison test between the case with $dt=10^{-11}$s did not show significant discrepancies. The reference parameters adopted for these simulations are reported in Table 1.

Part of the plasma is charged immediately at the beginning of the calculation whereas the most is produced in the plasma source region as previously reported.

The source walls' characteristics can be chosen by adopting three OOPIC objects: conducting surface with constant potential, dielectric and dielectric without the charges accumulation. This last configuration represents a non confining wall. The effects of the source walls on the plasma potential are shown in Fig 4 where Table 1 applies. Fig 5 shows the axial potential and potential lines for dielectric and biased left source walls.

Successively we evaluated the effects of particles' temperatures. Ions temperature does not change significantly the plasma potential, which increases with the electrons temperature as reported in Fig 6.

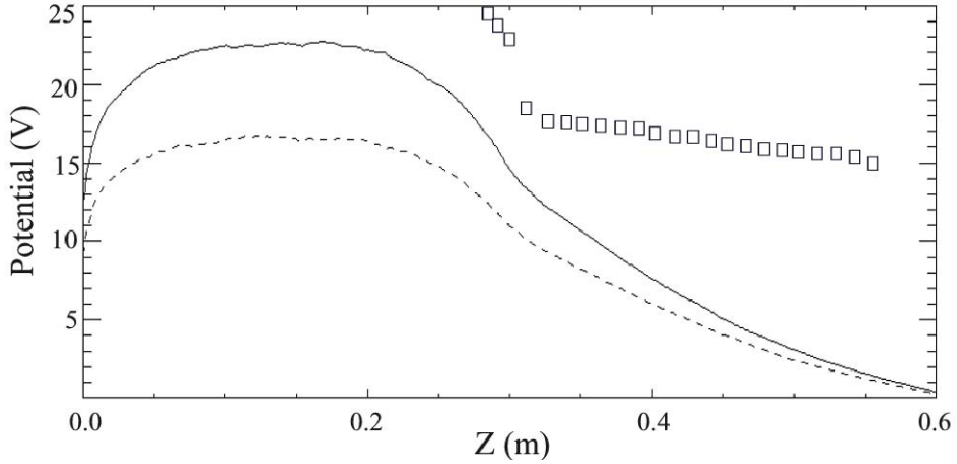

Figure 6. Plasma potential for different electrons' temperatures. *Comparison of axial plasma potentials for Te=9 and Te=5 eV (dash). Source rate of 5 10^{18} $m^{-3}s^{-1}$ and final density N_{ions}~10^{13} m^{-3}. The squares represent the Plihon measurements (Te=4.5eV and electronegative ions).*

Figure 7 should represent the IEDF measurements made by Charles and reported in Fig 2. It is shown that the greater percentage of the ions inside the expansion chamber and at the source axis has velocities between 4 and 5 10^4m/s, whereas for higher radius the peak velocity decreases to 3-3.5 10^4m/s. The ion sound speed for hydrogenous and Te=7eV is $\sqrt{(k\ Te/m_i)}$~2.5 10^4m/s, so the peak velocity for r~0 is around two times C_s as reported by Charles and Plihon. Figure 8 shows the percentage of axially trapped and reflexed particles. Very few reflexed electrons have been detected.

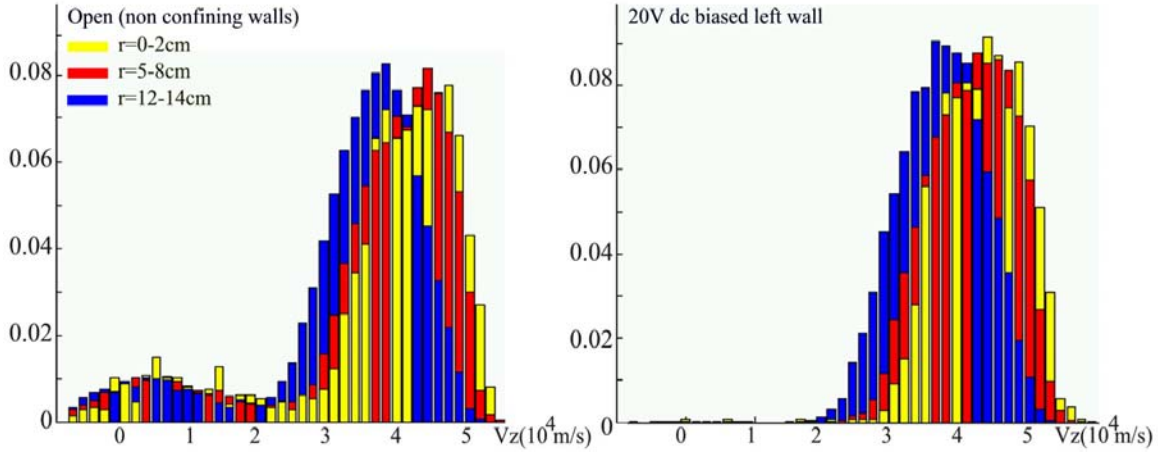

Figure 7: Axial velocity distributions. *The ions axial velocities is around two times the ions sound speed for radii lower than the source width. For higher radii most of the ions have lower axial velocities*

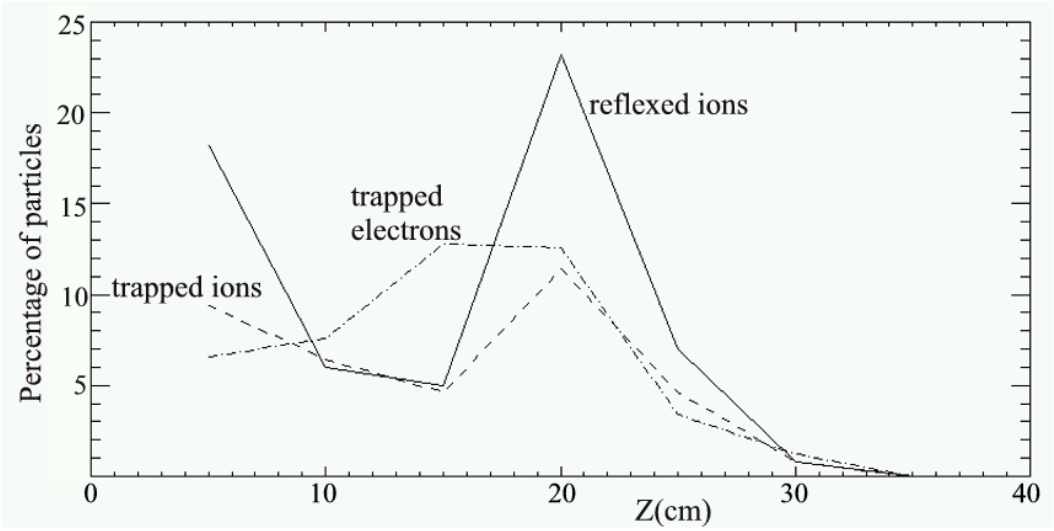

Figure 8: Trapped and reflexed ions and electrons. *Percentage of reflexed (Vz<0) and trapped (-500<Vz<500m/s) particles inside the helicon source.*

During the experiments the potential jump disappeared for pressures above 3-5 mTorr. Our simulations show a similar effect but for pressure greater than 100mTorr, so two orders of magnitude higher. The discrepancy can be explained considering that the real ions' density inside the helicon source was between 10^{15} and 10^{16} m^{-3} whereas for our studies we obtained values significantly lower: around 5 10^{12} m^{-3}. In fact the potential jump reduction happens for similar values of Ni x Nn, which scales the ionization factor (see Fig 9).

V. Fine grid simulations

Trying to increase the plasma production rate we have halved the spatial step in order to allow a higher plasma density. The nodes number went from 128x512 to 256x1024. The electrons temperature has been set at 6eV while ions at 0.01eV. We have simulated the most interesting cases: source tube completely made of dielectric and a

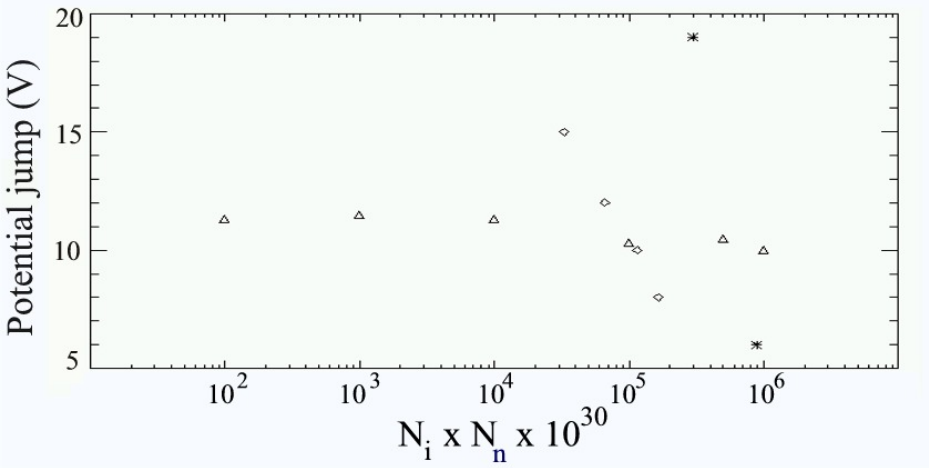

Figure 9: Potential jump as function of the ions times neutral pressures. *The potential jump of the OOPIC simulations (triangles), measured as maximum potential difference for z between 0.2 and 0.4 m, is compared with the Plihon (squares) and Charles (stars) measurements.*

conducting DC biased left wall. The simulations have been repeated changing the plasma generation rate in order to obtain a stable density which has been found at $5\ 10^{14}$ m^{-3} by adopting a source rate of $2\ 10^{19}$ $m^{-3}s^{-1}$. Fig 10 shows simulated and measured axial potentials: it appears that the potential jump is smooth and not as deep as during the experiments.

VI. Detachment and thrust

To evaluate the performances in space and the ions detachment we have increased the chamber dimension by maintaining the node numbers of the denser grid simulations (256x1024) and we enlarged the spatial step by returning to the value of 1.2mm. In this way we obtained a expanding chamber 1.2 m long, but we had to perform low density simulations returning to source rates of the order of $10^{18}m^{-3}s^{-1}$.

The plasma ions are again H because with Ar the sound speed decreases too much and the time necessary to fill the diffusion chamber is prohibitively high. Than we adopted two configurations for the diffusion chamber walls: grounded conductors and open surfaces.

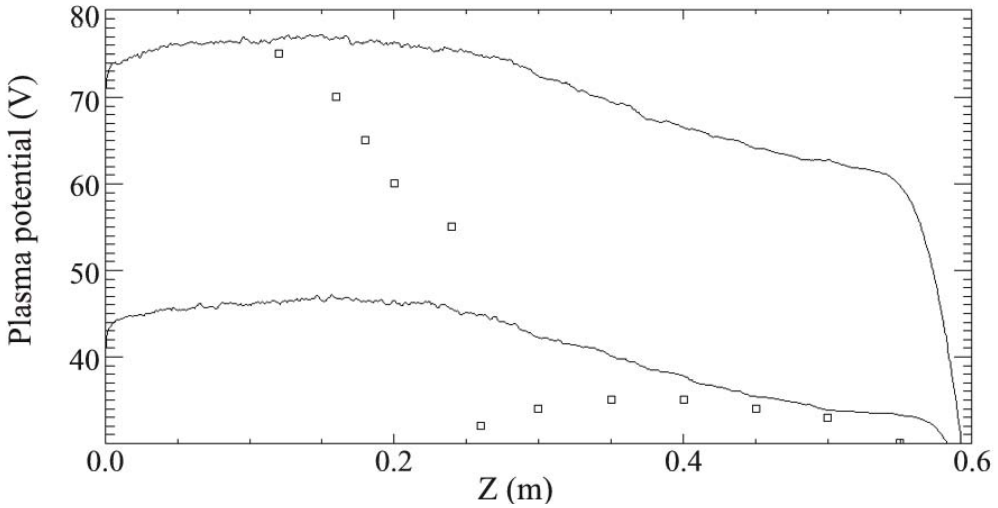

Figure 10: Simulated axial potential for 70 and 40 V biased left wall and measurements. *Axial potential after 22μs for dielectric source tube and conducting left source wall biased at 70 and 40 Volts. The plasma source rate is 2 $10^{19}m^{-3}s^{-1}$ which provide a stable density of 5 $10^{14}m^{-3}$ inside the helicon. The Charles measurements are reproduced as squares.*

To evaluate the detachment from the magnetic field lines we have analyzed the ions' trajectories inside the diffusion chamber. The particle velocity is curvilinear until the magnetic field acts on it, after a certain distance from the source the trajectory starts to be almost rectilinear, there we can suppose the detachment takes place. We argued that the detachment is function of the radius and it happens not before z of 0.7 and 1.2 m respectively for r=0 and 15 cm, so not before a distance between 0.4 and 0.8 m from the source tube.

Ones defined the minimum distances where the detachment should happen, we choose four reference lines at greater distances where evaluate thrust and specific impulse. Our goal was a parametric evaluation of the thruster's performances for different hypothetical detachment positions. The detachment lines have been defined as the z positions where, at a constant r, the ions' speed direction changes of less than 2 (lines 1 and 2), 6 (line 3), and 8° (line 4) for greater z. These schematic lines are reproduced in Fig 11.

For all the cells that follow the selected detachment line, we have evaluated the ions' density, which is a default output of OOPIC, and the average ions' axial velocity. Then, applying Eq. (1) and Eq. (2), we evaluated thrust and specific impulse. There m is the ion mass (H), N is the density of ions inside the detachment cell at radius r_i, Va is the average axial velocity inside the detachment cell, A is the cross surface of the cell revolution along $\varphi = \pi [(r_i+dr)^2-r_i^2]$ and N_m is the number of cells along the radius.

$$T = \sum_{i=1}^{Nm} m \cdot N_i^{\det} \cdot (Va_i^{\det})^2 \cdot A_i \tag{1}$$

$$I_S = \frac{\sum_{i=1}^{N_m} N_i^{\det} \cdot Va_i^{\det}}{\sum_{i=1}^{N_m} N_i^{\det}} \frac{1}{g} \tag{2}$$

The results are reported in Table 2, those are averages of three simulations made with Te=8eV, 70V biased left wall and diffusion chambers represented by open or grounded walls. The simulations we made reached a density, inside the source tube, around 5 $10^{13}m^{-3}$, the source rate has been set at 10^{18} and 3 $10^{18}m^{-3}s^{-1}$.

Table 2: Thrust and Specific Impulse evaluation

Detachment line	Ions	Specific Impulse (s)	Thrust (N)
1	H	2800	2E-9
2	H	2900	3E-9
3	H	3600	7E-9
4	H	4000	2E-8

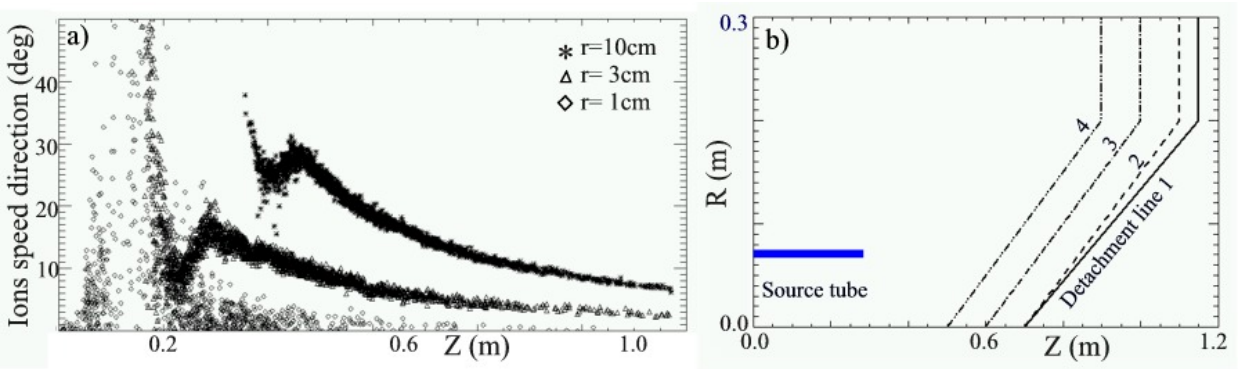

Figure 11: Ions speed directions and detachment lines. *The ions trajectories start to be rectilinear after 0.4 and 0.8 m from the source tube, depending on their radial positions (a). The detachment lines have been defined as the positions where the speed directions change less than 2, 6 and 8 degrees going to the right wall of the diffusion chamber.*

VII. Conclusions

The simulations have shown the formation and evolutions of plasma potential and ions axial velocity. The jump on the potential has not been seen as deep as reported but an ion flux at two times the ions sound speed has been obtained, in accordance with the bibliography.

The source walls, in particular the left one, have a great influence on the potential reached by the plasma. A conducting left wall biased at a sufficiently high potential can significantly increase the value registered inside the source tube and, sometimes, influence the stabilization of the plasma density there.

By increasing the neutral pressure it is possible to switch off the high energy ion flux and reduce the potential jump. These effects happen at pressures greater than the measured but at almost the same value of N_i x N_n (neutral particles density times ions density) which is directly proportional to the ionization factor.

Finally we evaluated the thrust and specific impulse, for H ions and source densities around 10^{13} m^{-3}, around 2 10^{-9} N and 3000 s. In this case the chamber length has been increased and the diameter till 1.2 m and 0.3m respectively, in order to allow a complete detachment.

Higher plasma density and higher chamber dimensions can be simulated by OOPIC only if it can be fully parallelized allowing a lower computational time.

References

[1] C. Charles, R.W. Boswell, "Laboratory evidence of a supersonic ion beam generated by a current-free helicon double-layer". Phys. Plasmas 11, 1706-1714 (2004).

[2] C. Charles, "Hydrogen ion beam generated by a current-free double-layer in a helicon plasma". Applied Physics Letters 84, 332-334 (2004).

[3] C. Charles and R.W. Boswell, "Current-free double-layer formation in a high-density helicon discharge". Applied Physics Letters 82, 1356-1358 (2003).

[4] N. Plihon, C. Corr, P. Chabert, "Double layer formation in the expanding region of an inductively coupled electronegative plasma", Applied Physics Lett, v86, 091501, (2005)

[5] N. Plihon, C. Corr, P. Chabert, "Periodic formation and propagation of double layers in the expanding chamber of an inductive discharge operating in Ar/SF6 mixture", Journal of Applied Phys, v98, 023306, (2005)

[6] J.P. Verboncoeur 1, A.B. Langdon 2, N.T. Gladd 3, "An object-oriented electromagnetic PIC code", Computer Physics Communications 87 (1995) pp199-211